A Randomized, Controlled Pharmacokinetic and Pharmacodynamics Trial of Ambrisentan After Fontan Surgery

Kevin D. Hill, MD, MSCI[1,2]; Anil R. Maharaj, PhD[2]; Jennifer S. Li, MD, MS[1,2]; Elizabeth Thompson, MD[1]; Piers C. A. Barker, MD[1]; Christoph P. Hornik, MD, PhD, MPH[1,2]

Objectives: To determine the pharmacokinetics, pharmacodynamics, and safety of the hepatically metabolized endothelin receptor antagonist, ambrisentan in children after Fontan surgery.

Design: Prospective, randomized, double-blind, placebo-controlled pharmacokinetic/pharmacodynamics and safety trial.

Setting: Single-center, postoperative cardiac ICU.

Patients: Children undergoing elective Fontan surgery.

Interventions: Subjects randomized on postoperative day number 1 to short-term (3 d) treatment with oral ambrisentan (2.5 mg in suspension, daily) versus placebo (4:1 randomization).

Measurements and Main Results: Plasma drug concentrations were measured at 0.5, 1, 2, 4, and 18–36 hours after the first dose. We developed a population pharmacokinetic model in NONMEM 7.2 (Icon Solutions, Ellicott City, MD) and applied the model to dose-exposure simulations. Pharmacodynamics endpoints were assessed at baseline and 3 hours after study drug administration, using postoperative hemodynamic monitoring lines. The analysis included 16 patients, 13 on ambrisentan (77 plasma samples); median age 36 months (range, 26–72 mo), weight 13.3 kg (11.1–17.6 kg), and nine males. There were no differences in baseline characteristics between ambrisentan and controls. A one-compartment model with first-order absorption and lag-time characterized the data well. Allometrically scaled weight was the only covariate retained in the final model. Typical values for clearance and volume of distribution were lower than previously reported in adults, 1 L/hr/70 kg and 13.7 L/70 kg, respectively. Simulated exposures with doses of 0.1–0.2 mg/kg approximated therapeutic exposures in adults with pulmonary arterial hypertension receiving 5 mg or 10 mg doses. Ambrisentan lowered plasma brain natriuretic peptide concentrations (452 ± 479 to 413 ± 462; $p = 0.046$), Fontan pressures (16.8 ± 2.9 to 15.6 ± 2.9; $p = 0.01$), and indexed pulmonary vascular resistance (2.3 ± 0.9 to 1.8 ± 0.6; $p = 0.01$) with no drug-related adverse events.

Conclusions: Ambrisentan clearance is reduced following Fontan surgery, perhaps reflecting abnormal hepatic metabolism in this population. The observed safety profile appears favorable and hemodynamic effects of ambrisentan may be beneficial for Fontan patients. (*Pediatr Crit Care Med* 2020; 21:e795–e803)

Key Words: ambrisentan; Fontan; pharmacodynamics; pharmacokinetics; pleural effusions; pulmonary vascular resistance

Pulmonary endothelial dysfunction is an important contributor to both short-term and longer-term morbidity in single ventricle patients after Fontan palliation. The in-series Fontan circuit is sensitive to the secondary increase in pulmonary vascular resistance that may result from endothelial dysfunction (1). Immediately following Fontan palliation, pulmonary endothelial dysfunction may contribute to prolonged pleural effusions (2–4) while, in the longer-term, endothelial dysfunction contributes to exertional intolerance and potentially Fontan failure (4–7).

Pulmonary endothelial modulators including the phosphodiesterase type-5 inhibitors, sildenafil, and udenafil, and the nonselective endothelin receptor antagonist (ERA), bosentan, have been studied in adolescents and adults with Fontan physiology. These drugs have generally shown positive results with improvements in exercise capacity and myocardial performance (4–9). However, there are limited data to support use of pulmonary endothelial modulators in Fontan patients in the immediate postoperative setting. In particular, no studies have evaluated the dosing, safety, or acute pulmonary vasodilating effect of ERAs. This is partly because ERAs mediate vascular remodeling and therefore are generally considered longer-term agents. It is also because bosentan, the most commonly used ERA in children, is potentially hepatotoxic (10), which is a major concern in Fontan patients due to their long term

[1]Division of Pediatric Cardiology, Department of Pediatrics, Duke University Pediatric and Congenital Heart Center, Durham, NC.

[2]Duke Clinical Research Institute, Durham, NC.

This article discusses off-label use of Ambrisentan after Fontan.

DOI: 10.1097/PCC.0000000000002410

risk of hepatic dysfunction (11, 12). As a selective endothelin-1 type A receptor antagonist, ambrisentan does not have any known hepatotoxicity (10), and may thus be beneficial in the immediate postoperative setting after Fontan. However, because ambrisentan is highly lipophilic, it may not compound easily in aqueous solution making it difficult to administer to younger children at time of Fontan palliation. Furthermore, ambrisentan undergoes primarily hepatic metabolism, which may be impacted by the unique Fontan physiology particularly in the immediate postoperative setting.

To address these knowledge gaps, we conducted a single-center, randomized, placebo-controlled trial (NCT02080637) to evaluate the pharmacokinetics, pharmacodynamics and safety of ambrisentan when administered as an aqueous solution via oral route to young children recovering from Fontan surgery.

MATERIALS AND METHODS

Patient Population

Subjects ages 24 to 120 months postnatal age with single ventricle heart defects undergoing Fontan surgery were potentially eligible for inclusion. Complete inclusion and exclusion criteria are included in the **supplemental materials** (**eTable 1**, Supplemental Digital Content 1, http://links.lww.com/PCC/B374). This study was reviewed and approved by the Duke University Medical Center Institutional Review Board.

Treatment

Subjects were randomized 4:1 to ambrisentan versus placebo with the small placebo control group intended to ensure unbiased collection of hemodynamic data by investigators. The sample size was appropriately powered for pharmacokinetics analysis and pre-/post-assessments but was not intended for placebo-controlled analyses. The treatment group received 2.5 mg of orally administered ambrisentan suspension prepared by an investigation pharmacist by crushing a 5 mg tablet and combining in 2.5 mL of Ora-plus solution and 2.5 mL of Ora-sweet solution. The placebo control consisted of 2.5 mL of Ora-plus combined with 2.5 mL of Ora-sweet and was not distinguishable from the treatment solution. Treatment was initiated on postoperative day number 1 (POD1) with repeated doses administered daily for up to three doses.

Data Collection

Baseline subject demographics (age, weight) and laboratory measures were recorded on POD1 prior to ambrisentan administration. Hemodynamic indicators were measured at baseline (i.e., post-Fontan surgery but pre-ambrisentan/placebo administration), and at 3 hours post-ambrisentan/placebo administration. Measurements and blood sampling were performed using "standard of care" central lines including an internal jugular line, common atrial line, and peripheral arterial line. Assessed indicators included superior vena cava pressure, common atrial pressure, mean arterial pressure (MAP), mixed venous oxygen saturation, and systemic arterial oxygen saturation and Pao_2. Standard Fick calculations were used to estimate pulmonary (Qp) and systemic (Qs) blood flows. Oxygen consumption (Vo_2) was estimated based on age and heart rate in children ages greater than or equal to 3 years. In those less than 3 years ($n = 6$), a Vo_2 of 160 mL/min/m^2 was used. The same Vo_2 was used for pre-study and post-study drug assessments. Indexed pulmonary and systemic vascular resistances were calculated in Wood units × m^2. Chest tube (CT) output was recorded hourly until CT removal. Plasma endothelin-1 and brain natriuretic peptide (BNP) concentrations were determined from plasma samples collected at baseline (post-Fontan, pre-ambrisentan administration) and at 3 hours post-ambrisentan administration from an internal jugular line. Pharmacokinetic samples were collected between 0 and 60 hours after administration of the first dose of study drug in all subjects (ambrisentan and placebo). In the treatment group, ambrisentan concentrations were quantified in plasma.

Analytic Methods

Concentrations of ambrisentan in human (sodium heparin) plasma were determined using liquid chromatography-tandem mass spectrometry at a commercial laboratory (Frontage, Exton, PA). Ambrisentan was extracted by protein precipitation using acetonitrile. Calibration standards and quality control samples were prepared in drug-free human plasma with sodium heparin. The lower limit of quantitation (LLOQ) was 2 ng/mL. The intra-assay accuracies of the quality control samples (2, 6, 60, and 1,500 ng/mL) ranged from 94.8% to 110.7%. Concentrations of endothelin-1 in human (sodium heparin) plasma were determined using a commercial enzyme-linked immunosorbent assay (Quantikine Endothelin-1 immunoassay, LLOQ 1 ng/mL; Frontage Labs, Hackensack, NJ). BNP levels were determined by the Duke Clinical Laboratory using a two-site immunoenzymatic ("sandwich") assay (LLOQ 1 pg/mL).

Population Pharmacokinetic Model Development and Evaluation

Detailed descriptions of the analytical methods and approach to model evaluation and validation are included in the supplemental materials (**eTables 1-4,** Supplemental Digital Content 1, http://links.lww.com/PCC/B374). Briefly, ambrisentan plasma concentrations were analyzed using nonlinear mixed-effects modeling approach with the software NONMEM 7.2 (Icon Solutions, Ellicott City, MD).

Based on visual inspection of data and literature review (13, 14), one- and two-compartment models were evaluated. Inter-individual variability (IIV) was assessed for pharmacokinetic model parameters using an exponential relationship (Equation 1). Estimation of a covariance matrix for IIV on clearance/inter-compartmental clearance (CL/Q) and volume (V) parameters was attempted.

$$P_{ij} = \theta_{Pop,j} \times \exp(\eta_{ij}) \quad (1)$$

Where P*ij* denotes the estimate of parameter *j* in the *i*th individual; $\theta_{Pop,j}$ is the typical population value for parameter *j*; and ηij denotes the deviation from the typical population value for parameter *j* in the *i*th individual. The random variable η is

assumed to be normally distributed with a mean zero and variance ω^2. Proportional, additive, and combined (proportional plus additive) residual error models were evaluated (Equations 2–4).

$$C_{obs,ij} = C_{pred,ij} \times (1 + \mu_{prop,ij}) \quad (2)$$

$$C_{obs,ij} = C_{pred,ij} + \mu_{add,ij} \quad (3)$$

$$C_{obs,ij} = C_{pred,ij} \times (1 + \mu_{prop,ij}) + \mu_{add,ij} \quad (4)$$

Where $C_{obs,ij}$ is the *j*th observed ambrisentan concentration in the *i*th individual; $C_{pred,ij}$ is the *j*th predicted concentration in the *i*th individual; $\varepsilon_{prop,ij}$ and $\varepsilon_{add,ij}$ are random variables with mean zero and variance $\sigma_{prop,ij}^2$ and $\sigma_{add,ij}^2$, respectively.

Body weight was a priori assumed to be a significant covariate for clearance and volume of distribution (allometric scaling) and was included in the base model prior to assessment of other covariates. The influence of additional covariates (e.g., serum creatinine, blood urea nitrogen, age, WBC count, hemoglobin, sex, and ventricular dominance [right vs left]) on the pharmacokinetics of ambrisentan was assessed using a univariate forward-backward elimination approach. A reduction of the objective function by 3.84 ($p < 0.05$) was required for inclusion of covariates during the forward step; an increase in the objective function by 7.88 ($p < 0.005$) was required for covariate retention during the backward elimination step. During the model building process, successful minimization, diagnostic plots, plausibility and precision of parameter estimates, condition numbers (ratio of the largest to smallest eigenvalues of the correlation matrix for parameter estimates), and objective function and shrinkage values were used to assess model appropriateness. Parameter precision of the final population pharmacokinetic (PopPK) model was evaluated using nonparametric bootstrapping (1,000 replicates) to generate 95% CIs for parameter estimates. Prediction-corrected visual predictive checks (pc-VPC) were generated from the base and final models using 1000 Monte Carlo (e.g., simulated) datasets based on the original study design (e.g., dosing, time of sampling) as described by Bergstrand et al (15). Last, normalized prediction distribution errors (NPDEs) were computed and analyzed as described by Comets et al (16).

Dose-Exposure Analysis

Post hoc estimates of steady-state ambrisentan exposures associated with enteral administration of a 2.5 mg dose every 24 hours were generated for treatment group subjects using the final PopPK model. Model estimates were compared with observed data from the literature depicting ambrisentan steady-state pharmacokinetics in pulmonary arterial hypertension (PAH) patients (children and adults) (13, 17). Steady-state estimates of ambrisentan exposure, calculated as the area under the concentration-time curve over the dosing interval ($AUC_{0–24, ss}$), among treatment group subjects were plotted against any covariates included in the final PopPK model to assess the extent of exposure changes over the range of covariate values. In addition, dose-exposure simulations following different single doses of ambrisentan were performed using 1,000 virtual children who were randomly generated based on the distribution of covariates among treatment group subjects. Simulations were based on the final PopPK model and included IIV on pharmacokinetic parameters. To assess the adequacy of prospective pediatric doses, simulated exposures, calculated as area under the concentration-time from 0 to infinity ($AUC_{0–\infty}$), were compared with steady-state exposure ($AUC_{0–24, ss}$) data from adult PAH patients who received Food and Drug Administration (FDA) approved doses, 5 and 10 mg (17). This comparison was considered appropriate based on previous literature indicating that ambrisentan displays time-independent pharmacokinetics (14, 17). Therefore, plasma exposures following single-dose administration ($AUC_{0–\infty}$) were expected to be equivalent to exposures at steady state ($AUC_{0–24, ss}$).

Adverse Events and Safety Measures

Total numbers of reported adverse events in both subject groups over the study period were classified based on the specific organ system and severity using the common terminology criteria for adverse events v4.0 (18). As treatment-related anemia is a common adverse event associated with ERAs, the percent change in hemoglobin between pre-ambrisentan/placebo administration and the lowest value observed during the treatment period (post-ambrisentan/placebo) was evaluated in both subject groups.

Statistical Analysis

The effect of drug treatment on specific hemodynamic indicators was graphically assessed through boxplots comparing placebo and treatment groups. A graphical comparison of weight-normalized CT outputs (mL/kg) collected over sequential 12-hour periods between placebo and treatment subjects was also shown. The outcome measure length of hospital stay (LOS) was summarized using measures of the central tendency (i.e., mean and median) and dispersion (SD and range) in both subject groups. The following descriptive statistics for subject demographics, dosing variables (e.g., number of doses), and laboratory measures were calculated: mean, SD, median, and range. The range denotes the minimum and maximum values of the data set. As only three children were allocated to the placebo group, statistical comparisons of demographic variables and laboratory measures between the placebo and treatment group ($n = 13$) were not performed. Comparisons of within-subject change in hemodynamic measures from baseline to 2 hours post-ambrisentan/placebo administration was performed using the nonparametric Wilcoxon signed rank test. All statistics, metrics, and graphical plots were computed in R (Version 3.4.3; R Foundation for Statistical Computing, Vienna, Austria) and RStudio (Version 1.1.383; RStudio, Boston, MA) with the lattice and ggplot2 packages.

RESULTS

Patient Population

Sixteen subjects were enrolled in the study and randomized (**Table 1**). Thirteen and three were allocated to treatment (i.e., ambrisentan) and placebo, respectively. The treatment group

TABLE 1. Clinical Data of Enrolled Subjects

Variable	Treatment Group ($n = 13$)	Placebo Group ($n = 3$)
Age (mo)	35 ± 7	48 ± 21
Weight (kg)	13.1 + 1.2	15.3 ± 2.5
Sex		
Male	7 (54%)	2 (67%)
Race		
White	10 (77%)	1 (33%)
Black or African American	1 (8%)	0 (0%)
Asian	1 (8%)	1 (33%)
Multiple races	1 (8%)	1 (33%)
Ethnicity		
Hispanic or Latino	1 (8%)	1 (33%)
Not Hispanic or Latino	12 (92%)	2 (66%)
Ventricular dominance		
Hypoplastic left heart	6 (46%)	0 (0%)
Hypoplastic right heart	7 (54%)	3 (100%)
Fontan type		
Extracardiac conduit	12 (92%)	3 (100%)
Lateral tunnel	1 (8%)	0 (0%)
Fenestrated Fontan		
Nonfenestrated	1 (8%)	1 (33%)
Fenestrated	12 (92%)	2 (66%)

Data are presented as mean ± SD or count (percentages).

included one additional subject enrolled as a "replacement" subject for hemodynamic assessments due to a dysfunctional internal jugular line in one of the originally randomized subjects. All study subjects received study drug on PODs 1 and 2. One subject randomized to ambrisentan declined his third dose of study drug.

Pharmacokinetics

Among the 13 subjects in the treatment group, 79 pharmacokinetic samples were collected from which plasma ambrisentan concentrations were quantified. Two samples were below the LLOQ (2 ng/mL) and were excluded from the analysis, leaving 77 samples for PopPK model development. The median (range) number of quantifiable pharmacokinetic samples per subject was 6 (4–7). Ambrisentan plasma concentrations-time data from treatment group subjects are displayed in **Figure 1**.

Population Pharmacokinetic Model Development and Evaluation. A one-compartment structural model was selected to describe the pharmacokinetics of ambrisentan. Detailed model development and evaluation criteria are described in the supplemental materials (Supplemental Digital Content 1, http://links.lww.com/PCC/B374). Final pharmacokinetic parameter estimates are shown in **Table 2**. Empirical Bayes (post hoc) estimated median (range) ambrisentan median clearance was 0.0223 L/hr/kg (0.0160–0.282 L/hr/kg). Weight normalized (to 70 kg) median (range) clearance was 1.00 L/hr (0.706–1.29 L/hr) with volume of distribution of 13.7 L/70 kg and half-life of 6.09 hours (4.81–8.49 hr).

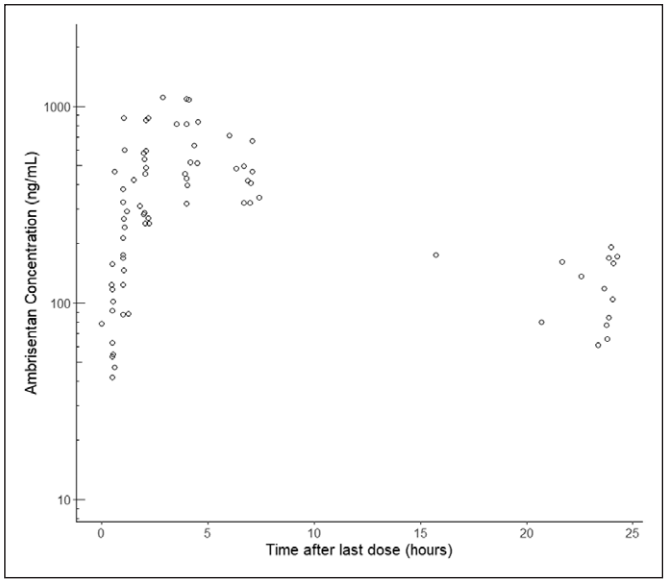

Figure 1. Plasma ambrisentan concentration versus time profile in children after Fontan.

The final pharmacokinetic model provided an appropriate fit to the data based on a pc-VPC which showed observed percentiles (5th, 50th, 95th) falling within model-based 95% prediction intervals for each respective percentile (**Fig. 2**). NPDEs generated from the final model displayed a mean and variance of 0.045 and 1.04, respectively (**eFig. 5**, Supplemental Digital Content 1, http://links.lww.com/PCC/B374), both consistent with a standard normal distribution based on statistical test (H_0: NPDE ~ N (0, 1); $p > 0.05$) and visual inspection of distribution (eFig. 5, Supplemental Digital Content 1, http://links.lww.com/PCC/B374).

Dose-Exposure Simulations. A comparison of steady-state pharmacokinetic parameter estimates between pediatric subjects from the treatment group and literature data from children with idiopathic or secondary PAH (13) is displayed in **Table 3**. Whereas time to reach the maximum concentration during the dosing interval (T_{max}) and terminal half-life were similar between both groups, the dose-adjusted maximum concentration during the dosing interval ($C_{max/dose}$) and the dose-adjusted exposure ($AUC_{0–24, ss/dose}$) were higher among the Fontan subjects reflecting reduced drug clearance. There was a trend toward increasing exposure ($AUC_{0–24, ss}$) with decreasing weight, most notably in subjects less than 13 kg (**eFig. 6**, Supplemental Digital Content 1, http://links.lww.com/PCC/B374).

A steady-state pharmacokinetic comparison between pediatric patients from the treatment group and literature data from adult PAH patients (17) is presented in the lower half of Table 3. Pediatric estimates were based on the study dose (2.5 mg), whereas observed data from adults reflect FDA recommended

TABLE 2. Parameter Estimates for the Final Population Pharmacokinetic Model for Ambrisentan

	Final Model		Bootstrap (n = 1,000)[a]		
Parameter	Estimate	RSE (%)	2.5th Percentile	Median	97.5th Percentile
Structural model					
ALAG (hr)	0.248	8.8	0.210	0.249	0.303
KA (hr^{-1})	0.385	25.3	0.124	0.382	0.627
$CL_{70\ kg}$ (L/hr)	1.00	7.2	0.872	1.01	1.17
$V_{70\ kg}$ (L)	13.7	8.9	5.84	13.7	16.15
$\theta_{CL,KA}$	−3.38	22.6	−9.17	−3.39	−1.19
Inter-individual variability					
IIV CL (coefficient of variation %)	19.4%	40.2[b]	6.1%	19.2%	31.2%
Residual error					
Proportional (%)	26.1%	23.9[b]	25.0%	18.7%	31.0%

ALAG = lag-time, $CL_{70\ kg}$ = population clearance estimate scaled to a 70 kg adult, IIV CL = inter-individual variability in drug clearance (shared with absorption rate constant), KA = absorption rate constant, RSE = relative SE, $V_{70\ kg}$ = population volume of distribution estimate scaled to a 70 kg adult, $\theta_{CL,KA}$ = ratio of inter-individual variability (SDS) between for clearance and absorption rate constant.

[a]Bootstraps estimates are representative of 999 model runs that achieved successful minimizations.

[b]RSE associated with the variance of the random-effect and removing unwanted variation estimate (e.g., ω^2 and ε^2).

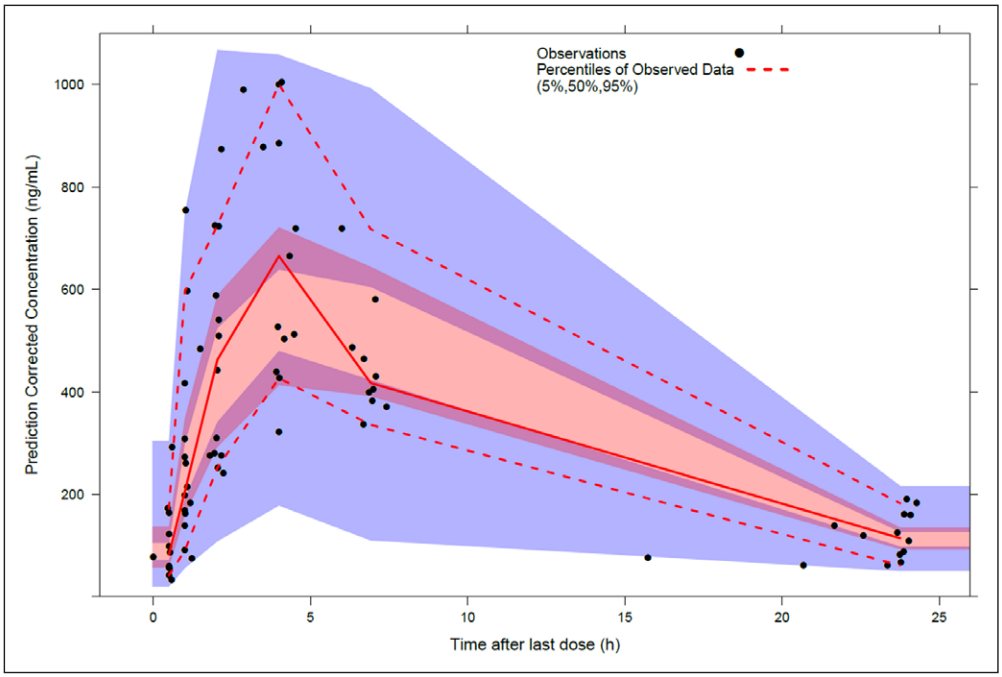

Figure 2. Prediction-corrected visual predictive check for the final population pharmacokinetic (PopPK) model. *Shaded areas* define 95% prediction intervals for the 5th (*blue*), 50th (*red*), and 95th (*blue*) percentiles based on 1,000 model simulations.

doses for adults (5 and 10 mg). Average estimates (geometric mean) of ambrisentan systemic exposure ($AUC_{0-24,\ ss}$) among pediatric Fontan subjects was ~1.8 × greater compared with adult PAH patients receiving 5 mg (17). Although based on a limited sample size (n = 2), observed exposure in adults receiving 10 mg appeared to be greater than our pediatric Fontan estimates for 2.5 mg. The average (arithmetic mean) terminal half-life of ambrisentan was longer in adult PAH patients compared with pediatric subjects from the current analysis.

Simulations from the final PopPK model using 1,000 virtual children whose weights were uniformly distributed with lower and upper limits reflective of treatment group subjects (11.1–15.9 kg), were employed to predict ambrisentan exposure following administration ($AUC_{0-\infty}$) of single 0.1 mg/kg and 0.2 mg/kg doses (**Fig. 3**). Simulated median (2.5th and 97.5th percentiles) exposures associated with 0.1 mg/kg and 0.2 mg/kg doses were 4,660 ng × hr/mL (3,205–6,590 ng × hr/mL) and 9,298 ng × hr/mL (6,428–13,133 ng × hr/mL), respectively. Comparison of simulated exposures from Fontan subjects to the above mentioned steady-state data from adult subjects with PAH (17), showed a good agreement between the 0.1 mg/kg pediatric and

TABLE 3. Comparison of Ambrisentan Steady-State Pharmacokinetic Between Children With Single Ventricle Cardiac Defects (Current Analysis) and Children With Pulmonary Arterial Hypertension (16) and Adult Pulmonary Arterial Hypertension Patients (19)

Source	*n*	Dose (mg)	Age (yrs)	Weight (kg)	Dose-Adjusted $C_{max/dose}$ (ng/mL/mg)	T_{max} (hr)	Dose-Adjusted $AUC_{0-24,\ ss/dose}$ (ng × hr/mL/mg)	Half-Life (hr)
Current analysis[a]	13	2.5	2.9 (2.2–4.2)	13.0 (11.1–15.9)	258 (174–448)	4.5 (2.5–6.2)	3,504 (2,748–5,636)	6.1 (4.8–8.5)
Takatsuki et al (13)[b]	15	5 (2.5–10)	9 (3–15)	30.2 (13.0–72.7)	114 (38.6–394)	3 (1–8)	1,000 (490–3,080)	7.05[c] (5.4–15.3)
Source	***n***	**Dose (mg)**	**Age (yr)**	**Weight (kg)**	**C_{max} (ng/mL)[f]**	**T_max (hr)[g]**	**AUC_{0-tau} (ng × hr/mL)[i]**	**Half-Life (hr)[i]**
Current analysis[d]	13	2.5	2.9 (2.2–4.2)	13.0 (11.1–15.9)	633.2 (30.8)	4.5 (2.5–6.2)	8,778.4 (23.6)	6.3 (4.8–8.5)
Food and Drug Administration clinical pharmacology biopharmaceutics review[e]	10	5	Adult	Adult	538.7 (36.6)	2 (1–3.1)	4,804.2 (37.4)	15.23[j] (7.9–31)
	3	10	Adult	Adult	1,146.8 (9.2)	2 (2–4)	12,591.3[h] (14.0)	12.9[j] (9.7–16.2)

$AUC_{0-24,\ ss/dose}$ = area under the concentration-time curve over the dosing interval/dose-adjusted exposure, $AUC0_{tau}$ = area under the concentration time curve from 0 to tau, C_{max} = maximum concentration, $C_{max/dose}$ = dose-adjusted maximum concentration during the dosing interval, T_{max} = time to reach the maximum concentration during the dosing interval.

[a]Derived from post hoc pharmacokinetic estimates for treatment group subjects based on the final population pharmacokinetic (PopPK) model.

[b]Pharmacokinetic analysis type (i.e., noncompartmental analysis) not depicted by the publication.

[c]*n* = 12 subjects (estimates of half-life missing for three subjects); half-life estimates based on study design with sampling over 24 hr after dosing.

[d]Derived from post hoc pharmacokinetic estimates for treatment group subjects based on the final PopPK model.

[e]Derived based on a two-stage pharmacokinetic analysis.

[f]Geometric mean (coefficient of variation).

[g]Median (minimum–maximum).

[h]Calculated based on *n* = 2.

[i]Arithmetic mean (minimum–maximum).

[j]Half-life estimates based on study design with sampling over 48 hr after dosing.

Data presented as median (minimum–maximum).

5 mg adult doses (adult geometric mean $AUC_{0-24,\ ss}$ = 4,804 ng × hr/mL). For a 0.2 mg/kg dose, pediatric simulations exhibited exposure values below those observed for adults receiving 10 mg (adult geometric mean $AUC_{0-24,\ ss}$ = 12,591 ng × hr/mL).

Pharmacodynamics

Hemodynamic Measures. Ambrisentan lowered Fontan pressures and indexed pulmonary vascular resistance but had no effect on common atrial pressures, cardiac index, or MAP. No change in any parameter was seen in the placebo group (Table 4).

Other Clinical Endpoints. Weight-normalized chest-tube output (mL/kg) following Fontan surgery was similar between placebo and treatment groups (**eFig. 7**, Supplemental Digital Content 1, http://links.lww.com/PCC/B374). The median (range) LOS was 8 days (7–20 d) and 10 days (7–24 d) in placebo and treatment groups, respectively ($p > 0.05$).

Biomarkers. For plasma BNP, 45 quantifiable samples were collected with a median of three samples per subject (range, 2–3). Pre- and 3 hours post-study drug samples were collected from all 16 subjects. When comparing baseline to 3 hours postdrug administration, ambrisentan subjects demonstrated significantly lower plasma BNP ($p = 0.046$; Table 4); BNP was lowered in 11 of 13 subjects. BNP increased in two out of three placebo subjects with a marginal decrease (101 to 97) in the third placebo subject. All subjects (placebo and ambrisentan) with BNP measured at 24–36 hours post study drug initiation demonstrated lowered BNP levels compared with baseline. Changes in endothelin levels (**eFigs. 8**, ***A*** and ***B***, Supplemental Digital Content 1, http://links.lww.com/PCC/B374) were generally consistent with an acute ambrisentan response but with no consistent observable pattern describing the pharmacokinetic/pharmacodynamics relationship between endothelin-1 and ambrisentan. Therefore, the development of a pharmacokinetic/pharmacodynamics model was not considered.

Safety

The number of reported adverse events over the study period, stratified by organ system, are reported in **eTable 5** (Supplemental Digital Content 1, http://links.lww.com/PCC/B374). There were no drug-related adverse events in either the treatment or placebo groups. Two ambrisentan subjects met reporting criteria for grade 1 anemia (hemoglobin < 10 g/dL) while no placebo subjects did. However, a similar percent decrease in hemoglobin from pretreatment to the lowest recorded value during the treatment phase was observed in both groups (median [range] percent decreases in hemoglobin were 5.44 [0–10.58%] and 4.65 [0–16.35%], for ambrisentan and

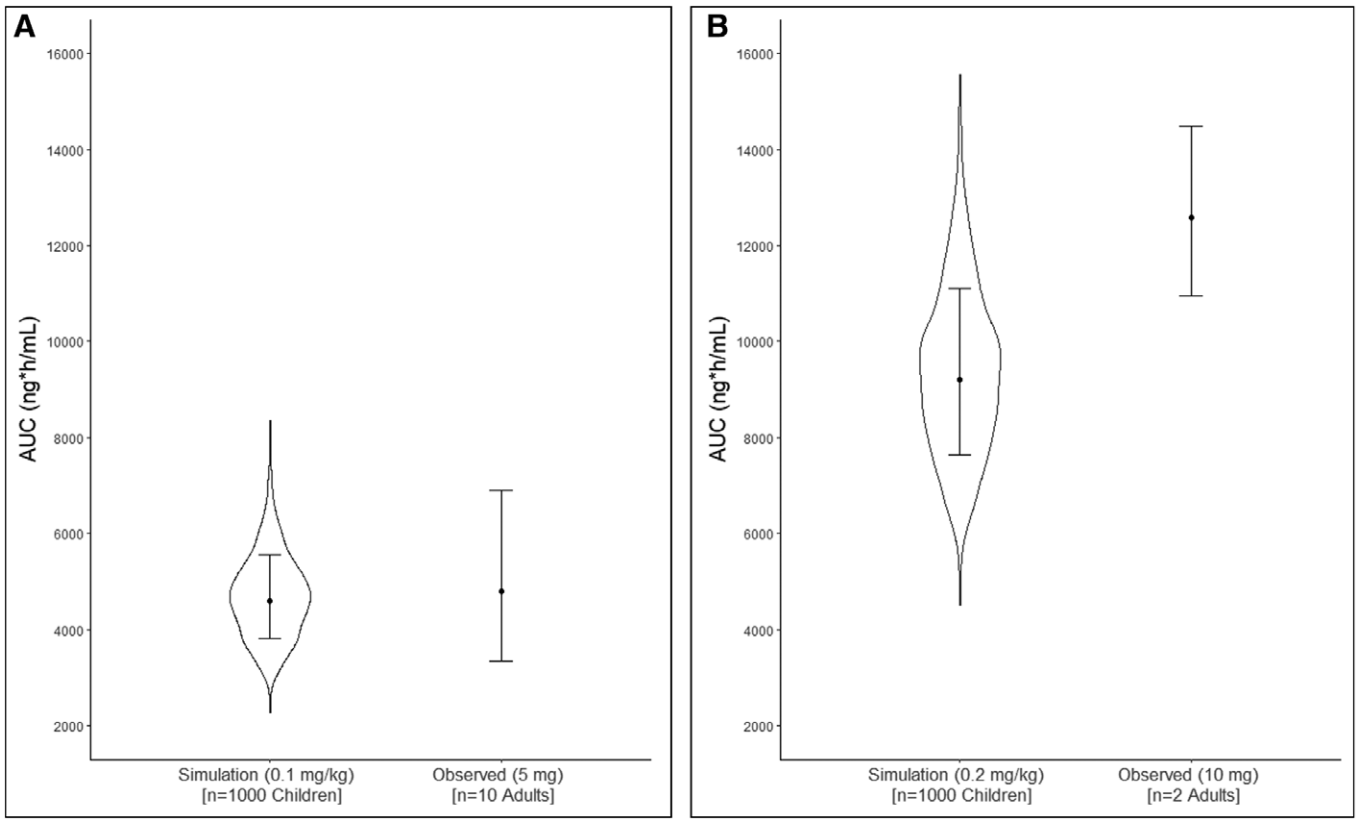

Figure 3. Simulated ambrisentan exposures. Following enteral administration of 0.1 mg/kg (**A**) and 0.2 mg/kg (**B**) doses in pediatric subjects with single ventricle heart defects ($n = 1{,}000$) compared with observed exposures from adult pulmonary arterial hypertension patients from the literature (17). For pediatric simulations, AUC represents the area under the concentration-time curve from zero in infinity ($AUC_{0-\infty}$) following single-dose administration. For observed adult data, AUC represents the steady-state area under the concentration-time curve over the 24 hr dosing interval ($AUC_{0-24\,hr,\,ss}$). *Points* represent the geometric mean of simulated and observed data. *Error bars* depict 1 geometric SD below/above the geometric mean. *Areas* (*violin plots*) depict the probability density of exposures associated with pediatric simulations. The *horizontal width* of each area is proportional to the density of data. AUC = area under the curve.

placebo, respectively). No subjects required blood transfusion after Fontan surgery and no subjects demonstrated clinically evident hepatic dysfunction.

DISCUSSION

The current analysis evaluated the population pharmacokinetics, pharmacodynamics, and safety of a compounded oral formulation of ambrisentan in children immediately after Fontan surgery. Ambrisentan was well tolerated. Despite concerns that the highly lipophilic drug would not compound effectively, we demonstrated good drug absorption with peak drug levels occurring ~4.5 hours after drug administration. Ambrisentan clearance was delayed when compared with older children with PAH translating to a dose-adjusted $AUC_{0-24,\,ss}$ approximately 3.5-fold higher in our Fontan subjects. Although this could be due to decreased relative efficiency of hepatic enzymatic metabolism in younger children (i.e., maturational effects), we speculate that, based on magnitude of the effect, this may more likely reflect impaired hepatic drug metabolism in postoperative Fontan subjects. We found that a dose of 0.1 mg/kg approximates the exposure seen in adults after a dose of 5 mg, the generally accepted treatment dose. Ambrisentan lowered pulmonary arterial pressures, pulmonary vascular resistance, and BNP. However, in this small study, we found no change in clinical endpoints including weight-normalized CT drainage or hospital LOS.

Ambrisentan Pharmacokinetics

A one-compartment structural model with first-order absorption (plus lag-time) and linear clearance appropriately described the data in our population. In comparison, previous studies in adults have depicted biphasic declines associated with ambrisentan plasma concentration-time profiles following oral administration, inferring that additional structural compartments may be required to adequately describe ambrisentan pharmacokinetic (14, 17). These prior studies employed protracted pharmacokinetic sampling schemes with samples collected greater than 24 hours after dose administration. In the current study, the final pharmacokinetic collection point was 24 hours after the last dose, limiting our ability to detect later changes to the concentration-time profile. Thus, based on the sampling scheme and trajectory of observed concentration-time profiles in our study, a one-compartment structural model was found to provide a reasonable fit.

It is notable that we found delayed ambrisentan clearance in our Fontan subjects when compared with previously published

TABLE 4. Hemodynamic Response to Study Drug Administration

Variable	Ambrisentan ($n = 12$)			Placebo ($n = 3$)		
	Baseline	3 hr Post drug	p	Baseline	3 hr Post drug	p
Fontan pressure (mm Hg)	**16.8 ± 2.9**	**15.6 ± 2.9**	**0.01**	14.3 ± 1.1	14.3 ± 1.1	1.0
Common atrial pressure (mm Hg)	9.8 ± 2.7	9.5 ± 2.6	0.41	7.0 ± 1.0	6.3 ± 0.6	0.16
Pulmonary vascular resistance index (Wood units × m^2)	**2.3 ± 0.9**	**1.8 ± 0.6**	**0.01**	1.8 ± 0.6	1.6 ± 0.1	0.59
Cardiac index (L/min/m^2)	3.5 ± 0.9	3.5 ± 0.8	0.31	4.1 ± 0.4	5.1 ± 0.9	0.29
Mean arterial pressure (mm Hg)	71 ± 9	72 ± 9	0.89	77 ± 2	72 ± 3	0.10
Brain natriuretic peptide	**452 ± 479**	**413 ± 462**	**0.046**	269 ± 242	305 ± 290	0.29

Boldface values are those that reach statistical significance ($p < 0.05$).

data from children with PAH (13). Delayed maturation is one possible explanation. However, based on the magnitude of effect (exposure increased ~3.5-fold) and age range of our patients, we speculate that postoperative Fontan physiology, with elevated central venous pressures and hepatic congestion, might have impacted hepatic clearance of ambrisentan. Both acute and chronic hepatic dysfunction are recognized concerns in Fontan patients (11, 12). We have previously shown markedly delayed clearance of sildenafil, another hepatically metabolized drug (20) in children after Fontan (21).

Ambrisentan Dosing and Formulation

Stochastic simulations based on our final PopPK model indicated dosage of 0.1 mg/kg in pediatric Fontan subjects would provide average (geometric mean) steady-state exposures ($AUC_{0–24, ss}$) congruent to that of adult PAH patients receiving 5 mg (19) (4,660 vs 4,804 ng × hr/mL, respectively). For a pediatric dosage of 0.2 mg/kg, the geometric mean $AUC_{0–24, ss}$ increased to 9,298 ng × hr/mL, a result which is consistent with the linear nature of clearance in the developed PopPK model. Previous studies in healthy adults support proportionate increases in ambrisentan exposure with escalating doses (14, 17). However, a small study including two adult PAH subjects demonstrated a disproportionate 2.6-fold increase in ambrisentan $AUC_{0–24, ss}$ with doses of 10 mg compared with subjects who received 5 mg (17).

Despite concerns that aqueous compounding of a highly lipophilic agent such as ambrisentan might not be feasible, all patients in our study demonstrated C_{max} and $AUC_{0–24}$ within the accepted therapeutic range in adults (14, 17). Thus, our compounding solution represents a reasonable approach for administering ambrisentan. These findings have implications for Fontan patients as well as the broader pediatric PAH population where ambrisentan use is typically limited to older patients capable of ingesting a tablet.

Ambrisentan Hemodynamic and Clinical Effects

This study was designed as a pharmacokinetic trial to assess appropriate dosing of ambrisentan after Fontan. A secondary objective was to assess immediate pharmacodynamics effects. A small placebo control group was employed with blinding to ensure that investigators collected and interpreted hemodynamic data in an unbiased manner. However, the study was not powered for placebo-controlled comparisons of drug effect, but rather to evaluate for predrug versus postdrug administration pharmacodynamics response. Notably, ambrisentan resulted in acute (within ~3 hr) lowering of Fontan pressures, pulmonary vascular resistance index, and plasma BNP levels. These are potentially important stand-alone findings, although the magnitude of effect was relatively small. In this underpowered (for placebo-controlled comparisons) study, we did not see clear evidence of clinical benefits with no change in hospital LOS or duration of CT drainage. It is generally accepted that lower PVRI is beneficial after Fontan surgery (1–4, 12) but no prior studies have demonstrated a benefit in terms of post-Fontan clinical endpoints.

There are notable limitations of the current analysis. As noted, the sample size was appropriate for pharmacokinetic analysis and pre-/post-assessments but was not intended for placebo-controlled analyses. We enrolled subjects with single right and single left ventricles, and by chance alone, all subjects in the placebo group had single right ventricular morphology (vs 7/13 of the ambrisentan subjects). Our study was not sufficiently powered for stratified analyses based on ventricular morphology. It is possible that the observed hemodynamic effects of ambrisentan simply represent improvements over time as patients recover from their Fontan surgery. Arguing against this, effects were seen within 3 hours of dosing, a time frame that corresponds to drug levels in the therapeutic range but is likely too short of a window to see spontaneous recovery of hemodynamic parameters. There are also well-described limitations of Fick calculations, particularly estimation of Vo_2 in younger children. We chose to use the same Vo_2 for pre- and post-assessments in an effort to standardize our assessments. With respect to the pharmacokinetic assessments, the major limitations of this study are associated with the narrow demographic range of assessed subjects and the study design.

First, the range of body sizes (e.g., weight) among the patient cohort was relatively narrow (11.1–15.9 kg). Second, the majority of pharmacokinetic samples (92.2%) were collected after the first dose. With PopPK modeling, the confidence instilled in model predictions is linked to the range of data used for model development. Therefore, the use of such models to generate predictions toward demographics (e.g., smaller or larger subjects) or dosing strategies (e.g., multiple dosing) outside the scope of data used to develop the model (i.e., extrapolations) should be conducted with appropriate discretion. In this analysis, model-based simulations of steady-state pharmacokinetics (e.g., multiple dosing) were computed based on the inference that ambrisentan pharmacokinetic is not altered with time. This inference was supported by literature data from healthy adults that denoted similar pharmacokinetic exposures between single-dose administration ($AUC_{0-\infty}$) and steady state ($AUC_{0-24,\,ss}$) (17, 19)
In conclusion, we describe the population pharmacokinetics of ambrisentan in pediatric subjects with single ventricle heart defects after Fontan palliation. Model simulations suggest an enteral dose of 0.1 mg/kg will provide similar exposures to that of adult PAH patients receiving 5 mg. The hemodynamic benefits of ambrisentan after Fontan surgery are potentially important but require further study to determine if these are sustained over time and to evaluate whether these benefits might translate into meaningful clinical benefits.

Supplemental digital content is available for this article. Direct URL citations appear in the printed text and are provided in the HTML and PDF versions of this article on the journal's website (http://journals.lww.com/pccmjournal).

This study was supported by a grant from the Gilead Cardiovascular Scholars Program, a grant from the Jackson Wall Family, and by a grant from the Trawick Pediatric Cardiology Research Fund supporting single ventricle research.

Drs. Hill and Li receive support from the National Centers for Advancing Translational Sciences for their work in pediatric drug development (U01TR-001803-01). Dr. Hornik receives salary support for research from National Institute of Child Health and Human Development (1K23HD090239), the National Heart, Lung, and Blood Institute (R61/R33HL147833), the U.S. Food and Drug Administration (1R01-FD006099, principal investigator [PI]: M. Laughon; and 5U18-FD006298, PI: D. K. Benjamin), the U.S. government for his work in pediatric clinical pharmacology (Government Contract HHSN275201800003I, PI: D. K. Benjamin under the Best Pharmaceuticals for Children Act), the nonprofit Burroughs Wellcome Fund, and other sponsors for drug development in adults and children (https://dcri.org/about-us/conflict-of-interest/). Drs. Hill's, Maharaj's, Barker's, and Hornik's institutions received funding from Gilead Sciences. Drs. Hill's and Barker's institution received funding from Jackson Wall Family and the Trawick Family Pediatric Cardiology Research Fund. Dr. Hill received funding from Sarfez Pharmaceuticals, and he received support for article research from the National Institutes of Health. Drs. Hill, Maharaj, Li, and Hornik disclosed off-label product use of ambrisentan after Fontan surgery. Dr. Maharaj received funding from Design2Code (consulting). Dr. Thompson has disclosed that she does not have any potential conflicts of interest.

For information regarding this article, E-mail: kevin.hill@duke.edu

The content in this article is solely the responsibility of the authors.

REFERENCES

1. Gewillig M, Brown SC: The Fontan circulation after 45 years: Update in physiology. *Heart* 2016; 102:1081–1086
2. Mascio CE, Austin EH 3rd: Pleural effusions following the Fontan procedure. *Curr Opin Pulm Med* 2010; 16:362–366
3. Mascio CE, Wayment M, Colaizy TT, et al: The modified Fontan procedure and prolonged pleural effusions. *Am Surg* 2009; 75:175–177
4. Yun TJ, Im YM, Jung SH, et al: Pulmonary vascular compliance and pleural effusion duration after the Fontan procedure. *Int J Cardiol* 2009; 133:55–61
5. Hebert A, Mikkelsen UR, Thilen U, et al: Bosentan improves exercise capacity in adolescents and adults after Fontan operation: The TEMPO (Treatment With Endothelin Receptor Antagonist in Fontan Patients, a Randomized, Placebo-Controlled, Double-Blind Study Measuring Peak Oxygen Consumption) study. *Circulation* 2014; 130:2021–2030
6. Rhodes J, Ubeda-Tikkanen A, Clair M, et al: Effect of inhaled iloprost on the exercise function of Fontan patients: A demonstration of concept. *Int J Cardiol* 2013; 168:2435–2440
7. Van De Bruaene A, La Gerche A, et al: Sildenafil improves exercise hemodynamics in Fontan patients. *Circ Cardiovasc Imaging* 2014; 7:265–273
8. Goldberg DJ, French B, McBride MG, et al: Impact of oral sildenafil on exercise performance in children and young adults after the Fontan operation: A randomized, double-blind, placebo-controlled, crossover trial. *Circulation* 2011; 123:1185–1193
9. Goldberg DJ, Zak V, Goldstein BH, et al; Pediatric Heart Network Investigators: Results of the FUEL trial. *Circulation* 2020; 141:641–651
10. Aversa M, Porter S, Granton J: Comparative safety and tolerability of endothelin receptor antagonists in pulmonary arterial hypertension. *Drug Saf* 2015; 38:419–435
11. Goldberg DJ, Surrey LF, Glatz AC, *et al*: Hepatic fibrosis is universal following Fontan operation, and severity is associated with time from surgery: A liver biopsy and hemodynamic study. *J Am Heart Assoc* 2017; 6:e004809
12. Rychik J, Veldtman G, Rand E, et al: The precarious state of the liver after a Fontan operation: Summary of a multidisciplinary symposium. *Pediatr Cardiol* 2012; 33:1001–1012
13. Takatsuki S, Rosenzweig EB, Zuckerman W, et al: Clinical safety, pharmacokinetics, and efficacy of ambrisentan therapy in children with pulmonary arterial hypertension. *Pediatr Pulmonol* 2013; 48:27–34
14. Yoshida S, Shirato K, Shimamura R, et al: Efficacy, safety, and pharmacokinetics of ambrisentan in Japanese adults with pulmonary arterial hypertension. *Curr Med Res Opin* 2011; 27:1827–1834
15. Bergstrand M, Hooker AC, Wallin JE, et al: Prediction-corrected visual predictive checks for diagnosing nonlinear mixed-effects models. *AAPS J* 2011; 13:143–151
16. Comets E, Brendel K, Mentré F: Computing normalised prediction distribution errors to evaluate nonlinear mixed-effect models: The npde add-on package for R. *Comput Methods Programs Biomed* 2008; 90:154–166
17. U.S. Food & Drug Administration: Letairis (Ambrisentan): Drug Approval Package. 2007. Available at: https://www.accessdata.fda.gov/drugsatfda_docs/nda/2007/022081s000TOC.cfm. Accessed January 1, 2020
18. National Cancer Institute: Common Terminology Criteria for Adverse Events (CTCAE). Available at: https://ctep.cancer.gov/protocolDevelopment/electronic_applications/ctc.htm. Accessed January 1, 2020
19. Galié N, Badesch D, Oudiz R, et al: Ambrisentan therapy for pulmonary arterial hypertension. *J Am Coll Cardiol* 2005; 46:529–535
20. Muirhead GJ, Rance DJ, Walker DK, et al: Comparative human pharmacokinetics and metabolism of single-dose oral and intravenous sildenafil. *Br J Clin Pharmacol* 2002; 53(Suppl 1):13S–20S
21. Hill KD, Sampson MR, Li JS, et al: Pharmacokinetics of intravenous sildenafil in children with palliated single ventricle heart defects: Effect of elevated hepatic pressures. *Cardiol Young* 2016; 26:354–362